CORRECTION NOTICE

Nat. Med. **22, 497–505 (2016)**

Genotype tunes pancreatic ductal adenocarcinoma tissue tension to induce matricellular fibrosis and tumor progression

Hanane Laklai, Yekaterina A Miroshnikova, Michael W Pickup, Eric A Collisson, Grace E Kim, Alex S Barrett, Ryan C Hill, Johnathon N Lakins, David D Schlaepfer, Janna K Mouw, Valerie S LeBleu, Nilotpal Roy, Sergey V Novitskiy, Julia S Johansen, Valeria Poli, Raghu Kalluri, Christine A Iacobuzio-Donahue, Laura D Wood, Matthias Hebrok, Kirk Hansen, Harold L Moses & Valerie M Weaver

In the version of this supplementary file originally posted online, the supplementary information file was incomplete and lacked some data in Supplementary Figure 11. The error has been corrected in this file as of 5 August 2016.

Supplementary Fig 1.

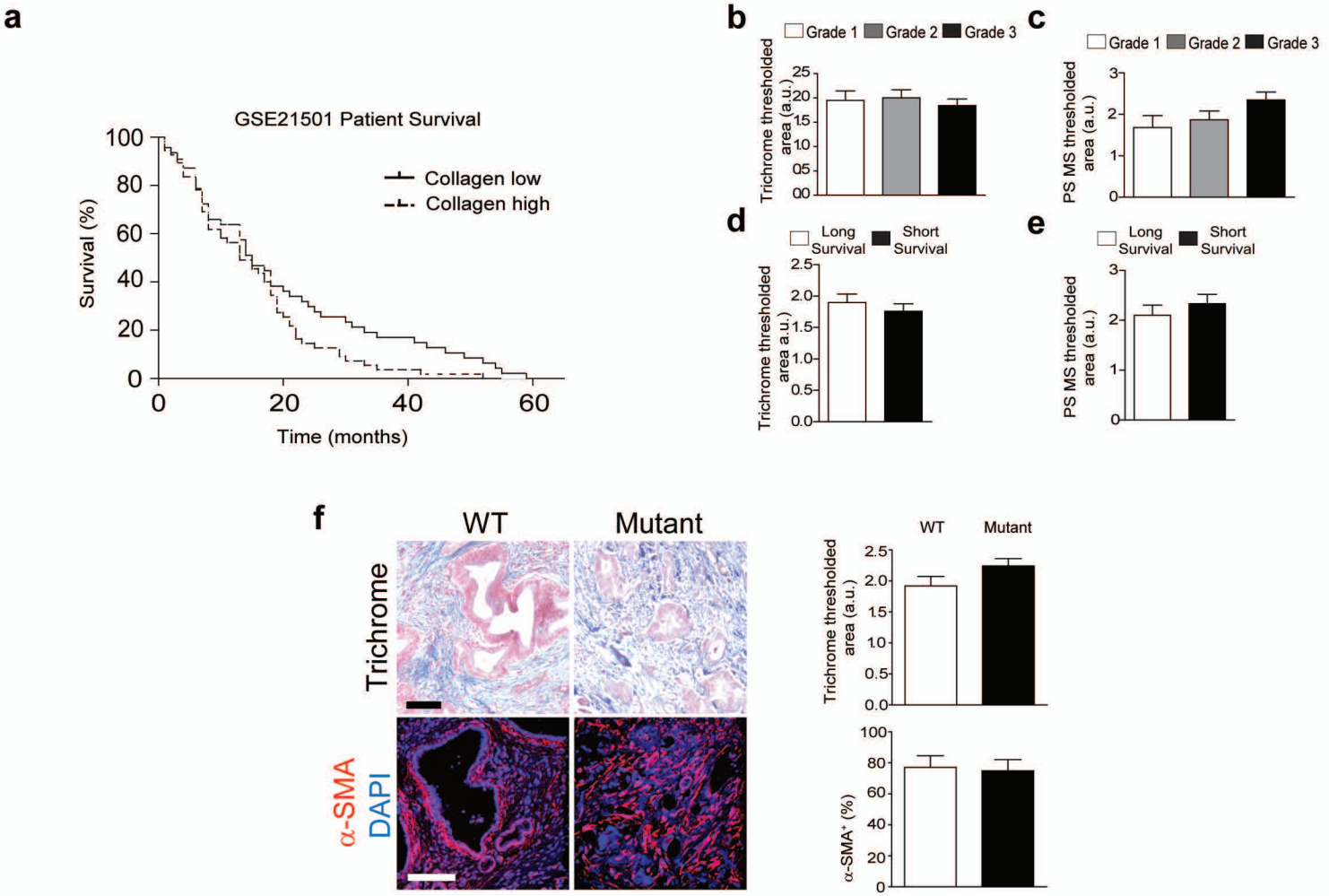

Supplementary Fig 2.

a

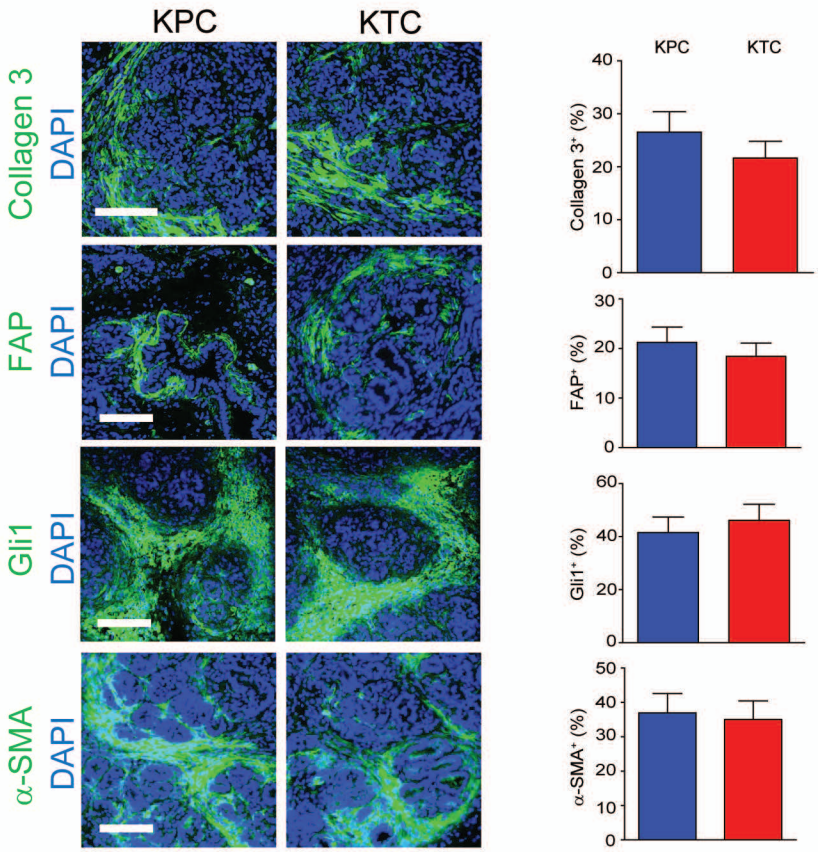

Supplementary Fig 3.

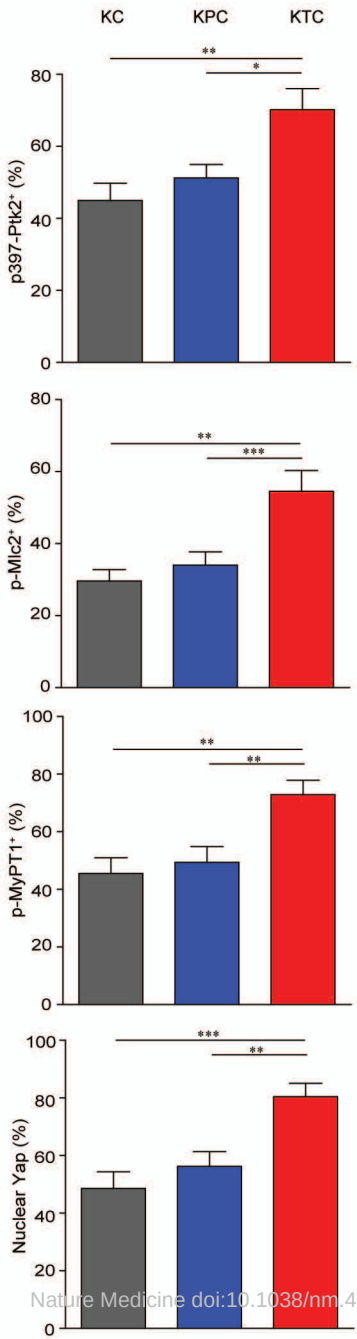

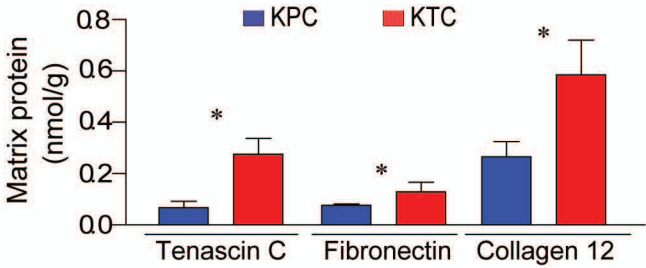

c

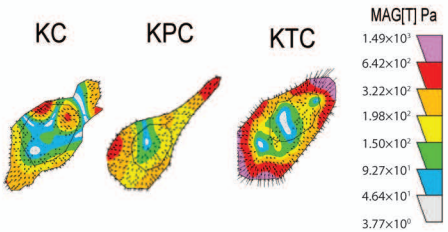

Supplementary Fig 4.

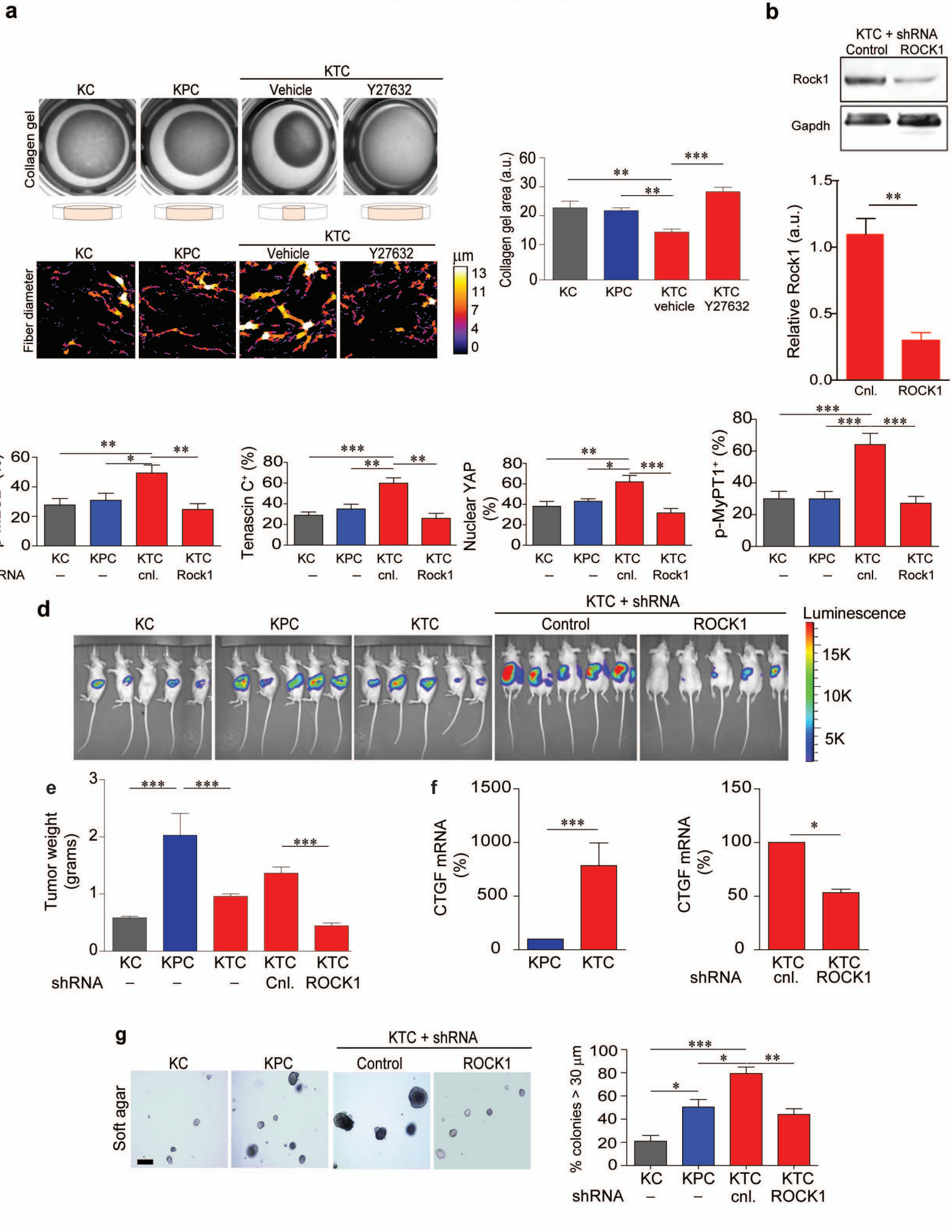

Nature Medicine doi:10.1038/nm.4082

Supplementary Fig 5.

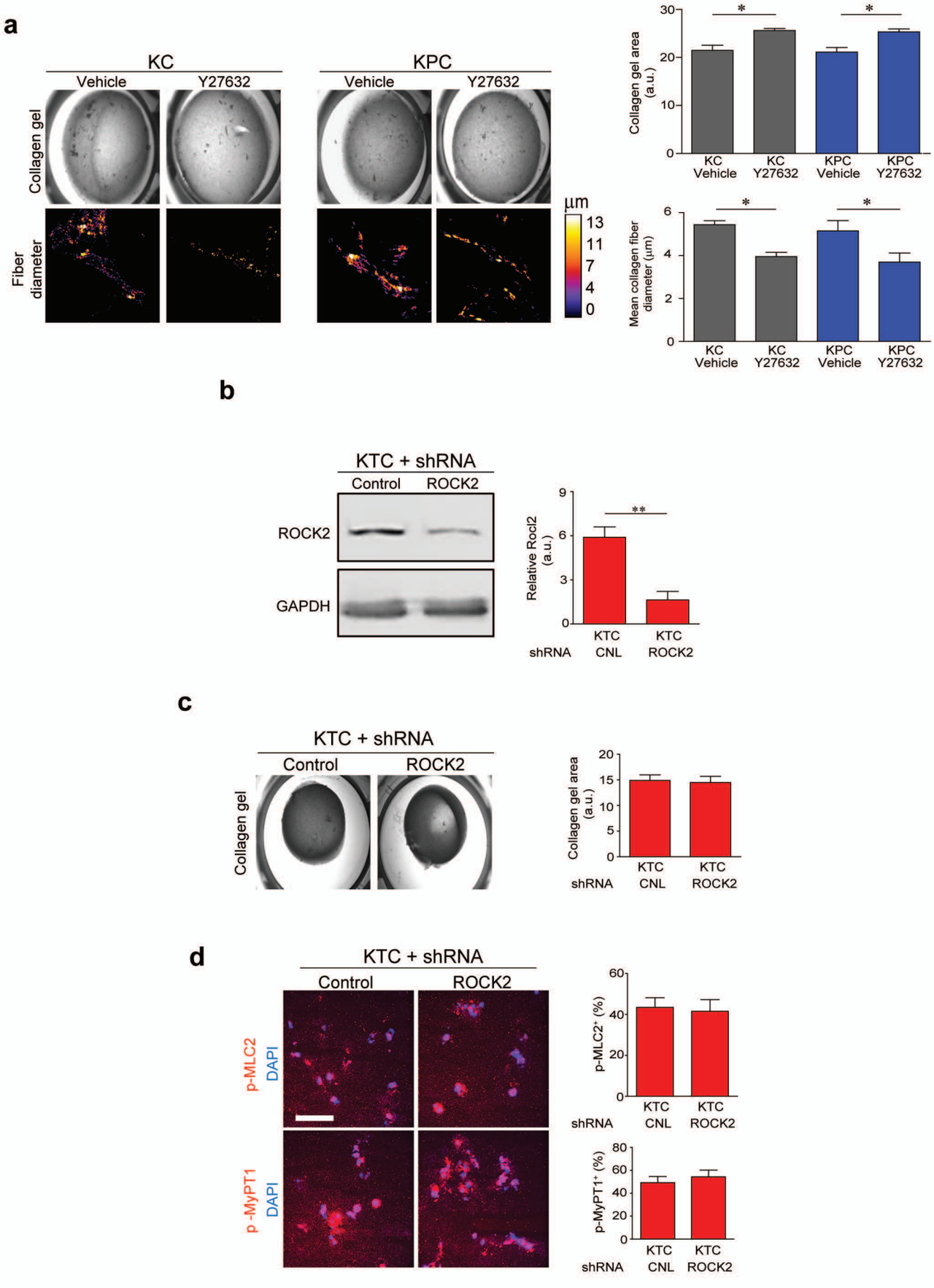

Nature Medicine doi:10.1038/nm.4082

Supplementary Fig 6.

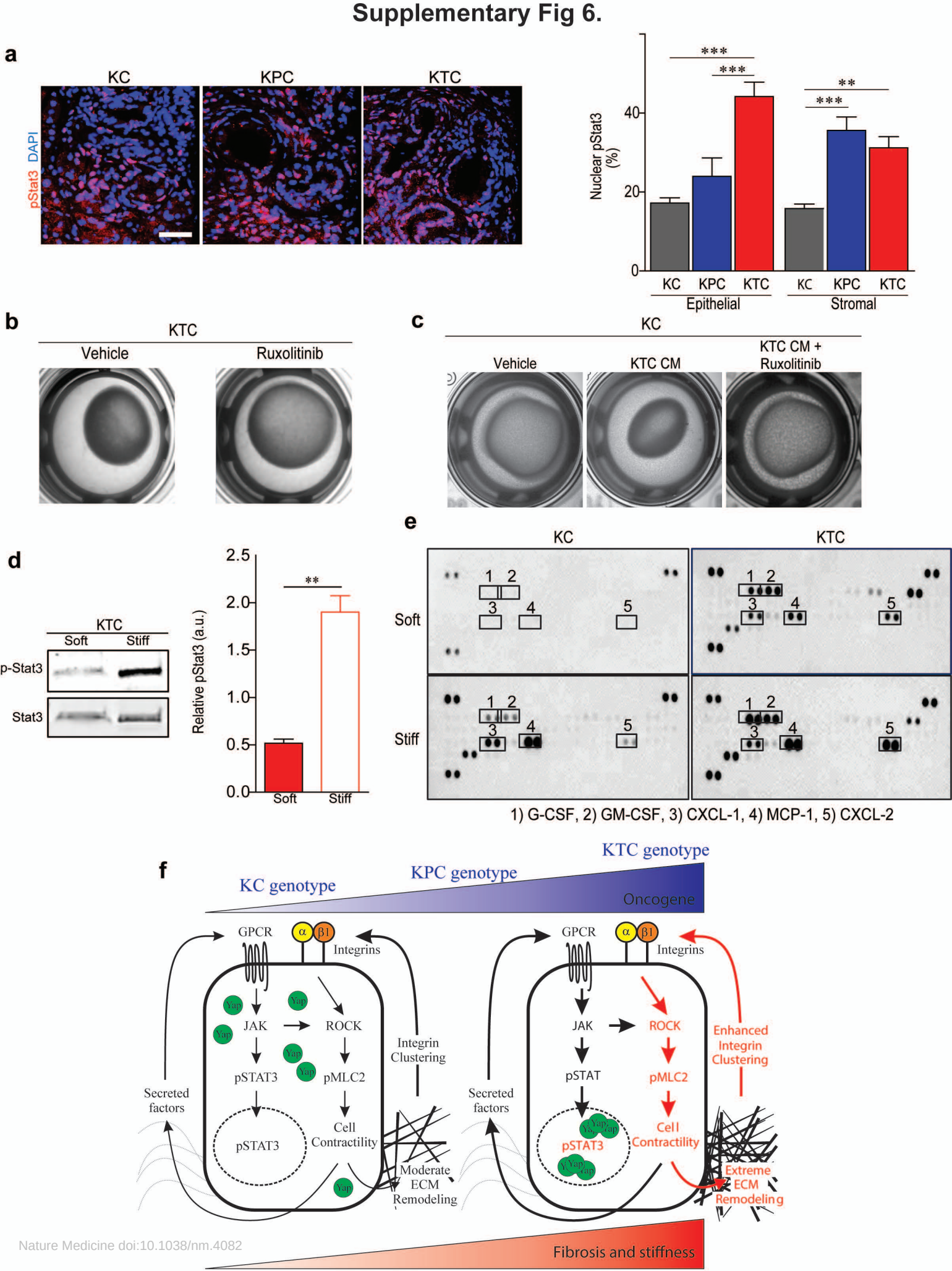

Nature Medicine doi:10.1038/nm.4082

Supplementary Fig 7.

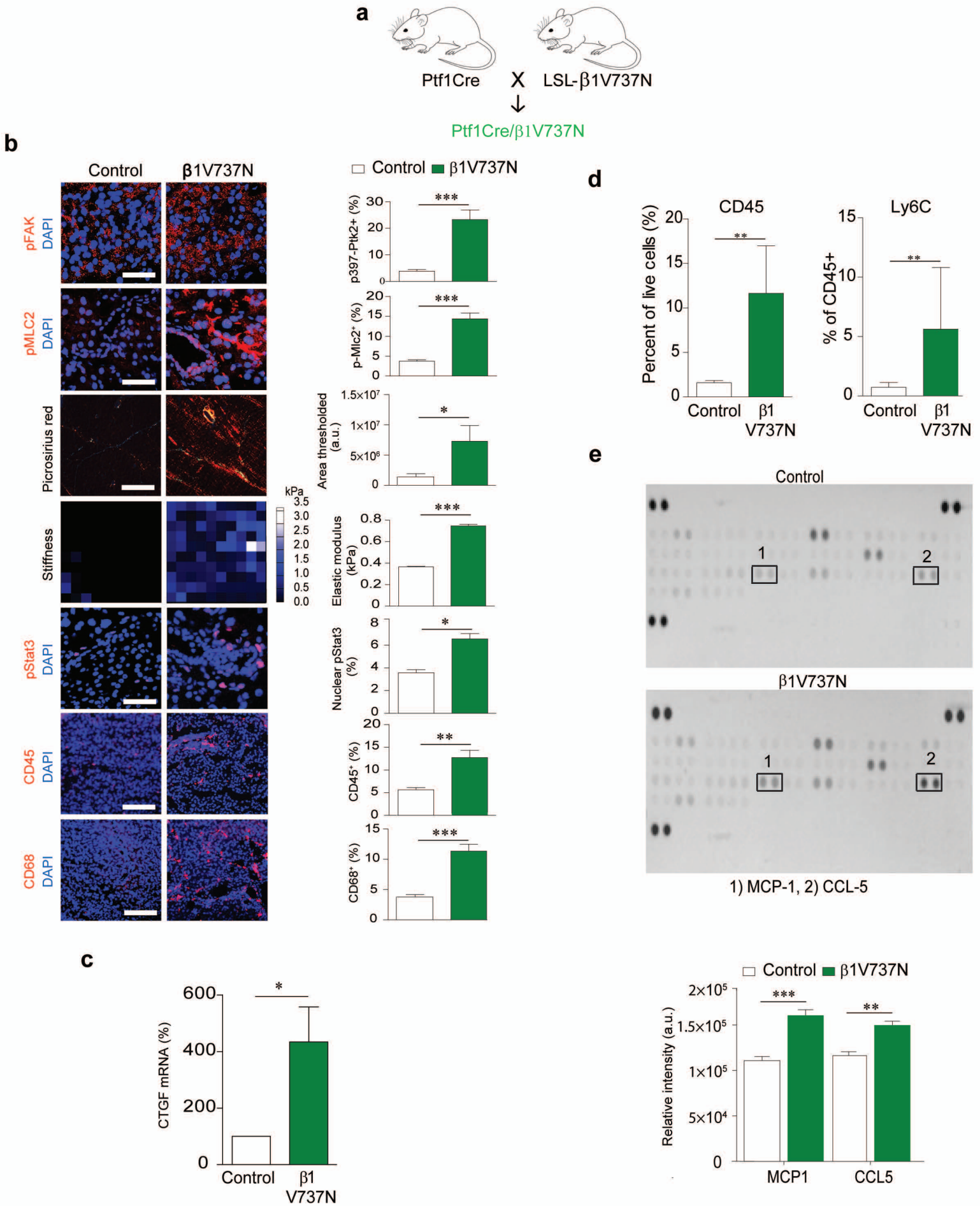

Nature Medicine doi:10.1038/nm.4082

Supplementary Fig 8.

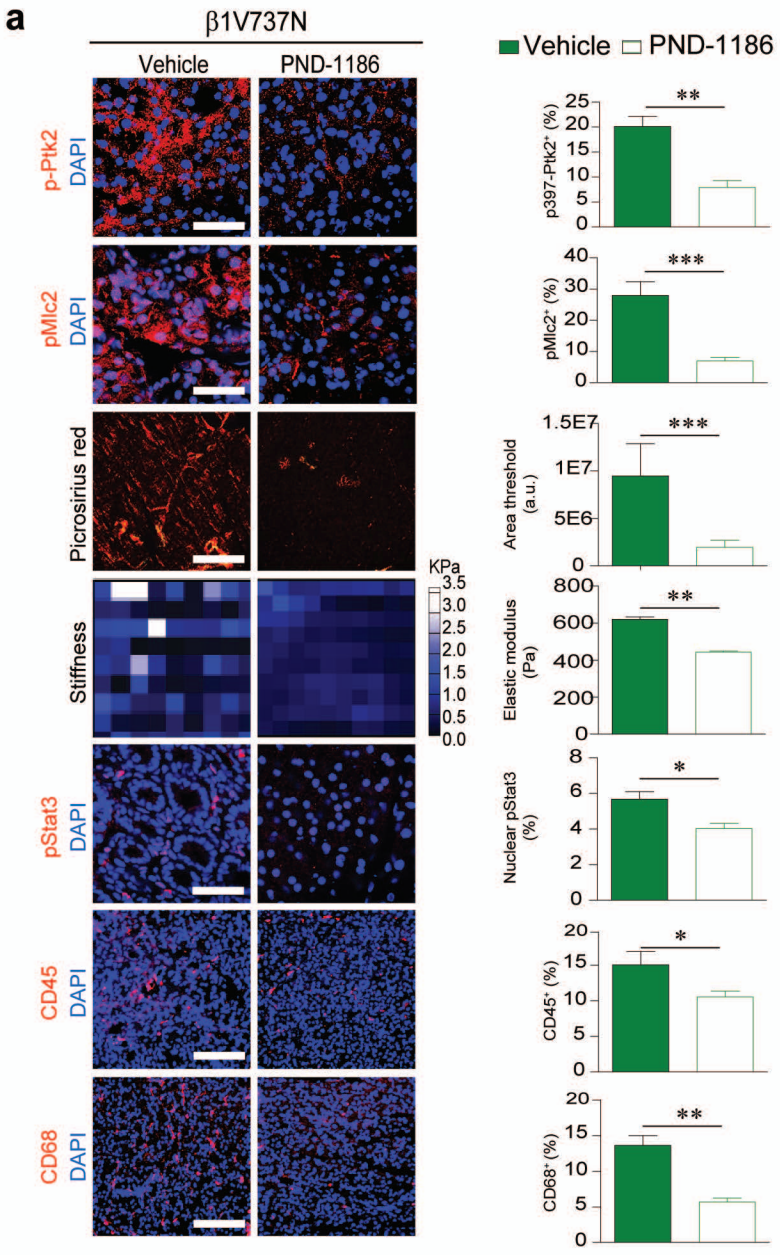

Nature Medicine doi:10.1038/nm.4082

Supplementary Fig 9.

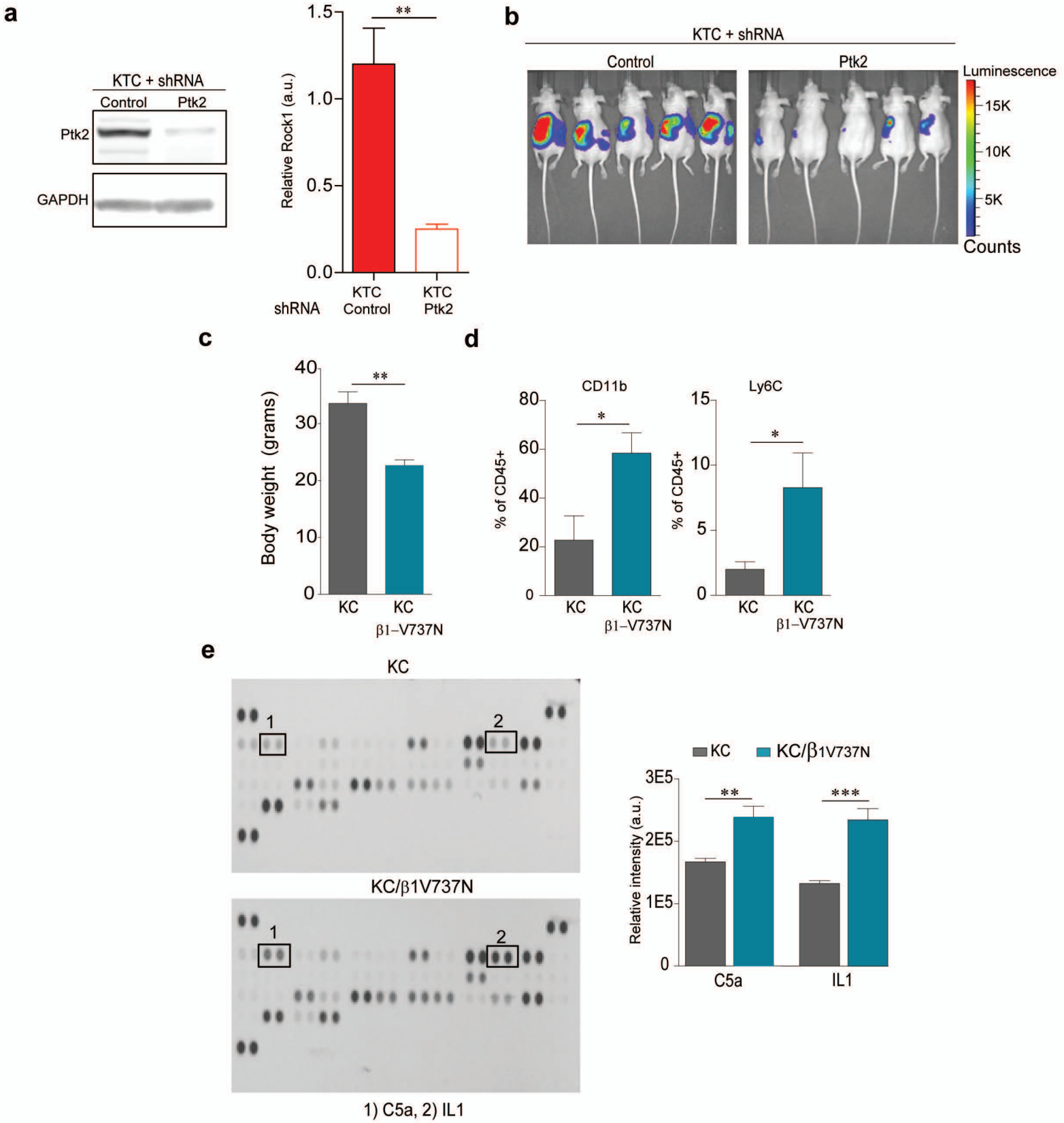

Nature Medicine doi:10.1038/nm.4082

Supplementary Fig 10.

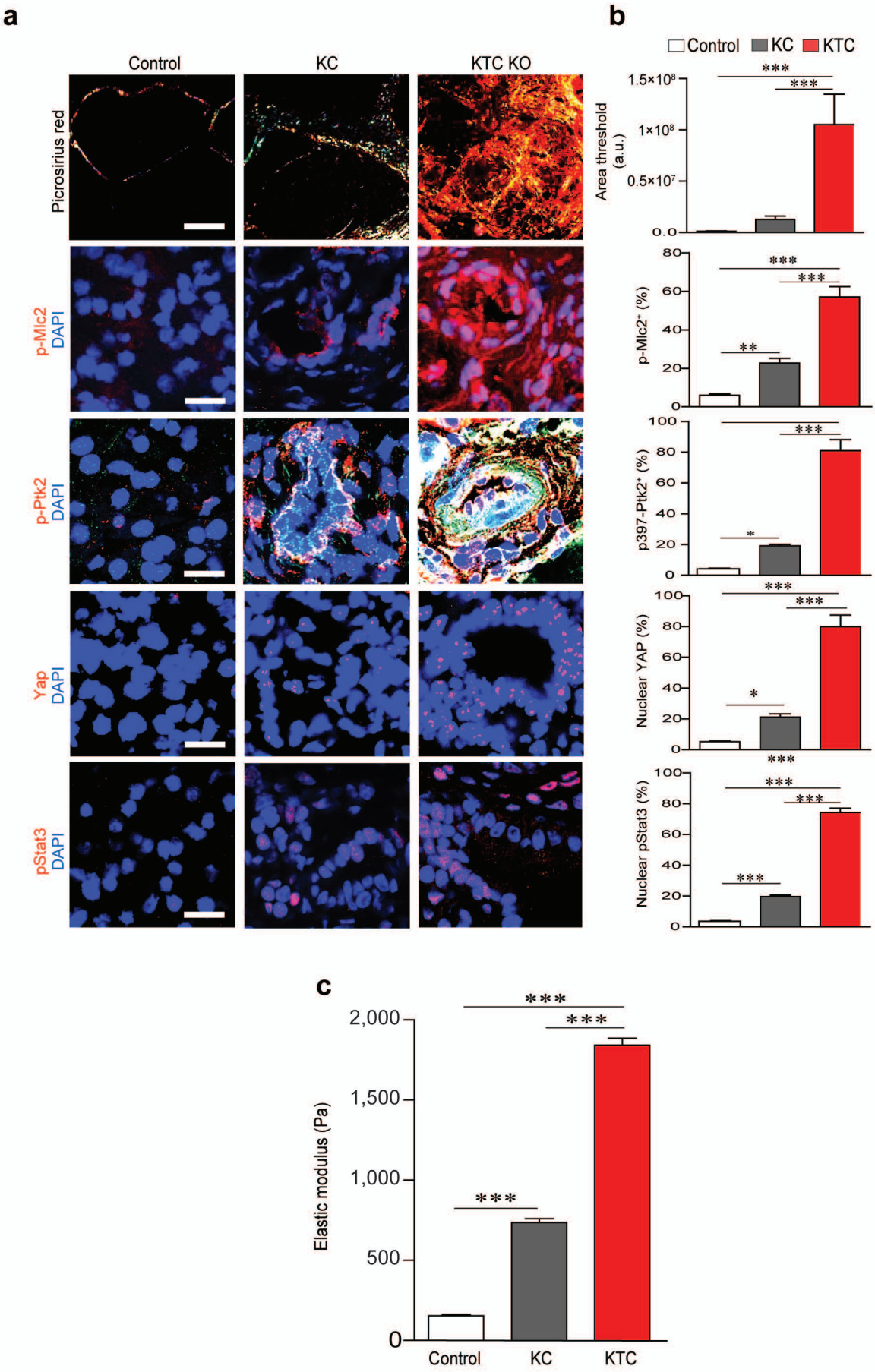

Nature Medicine doi:10.1038/nm.4082

Supplementary Fig 11.

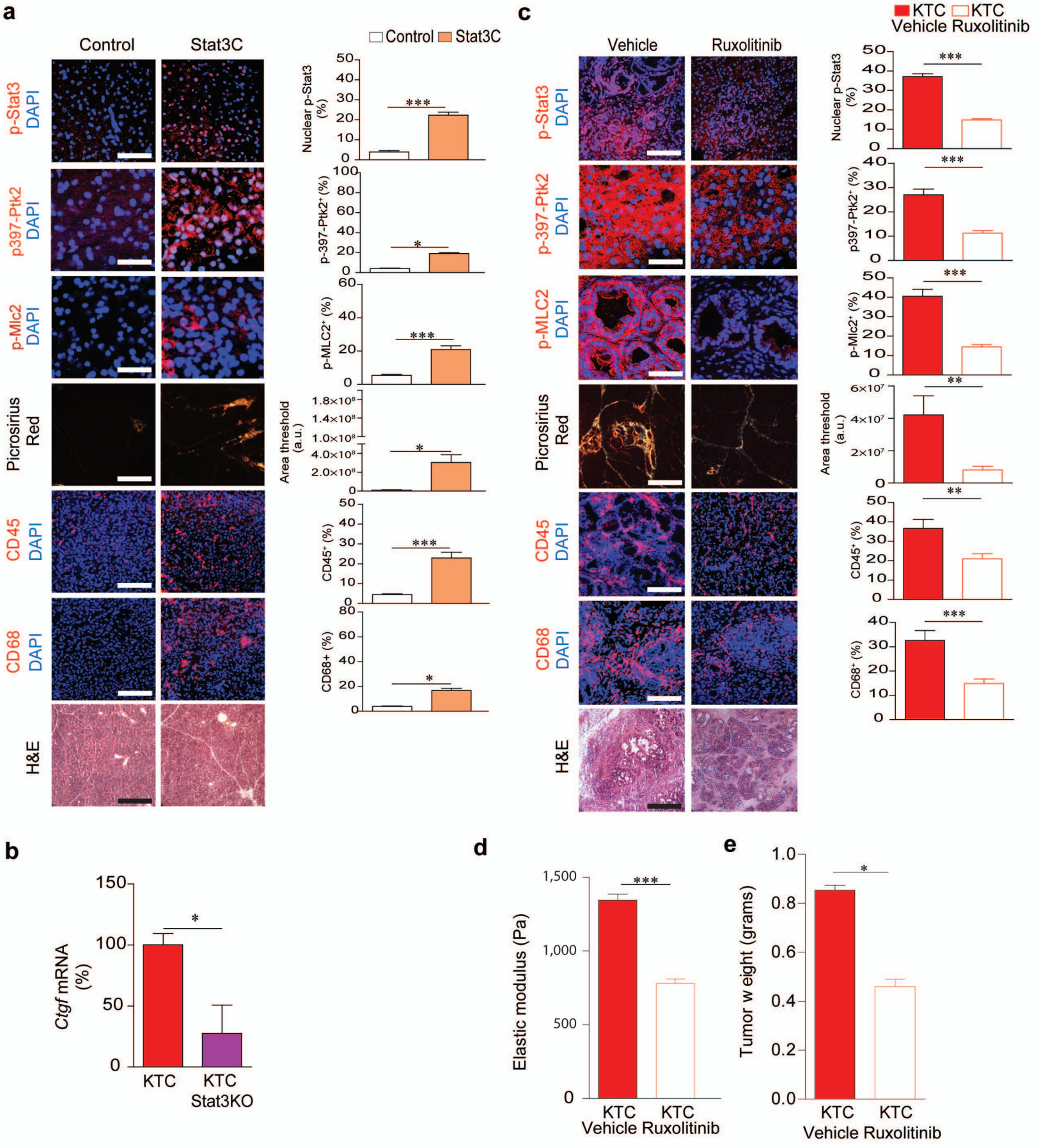

Supplementary Fig 12.

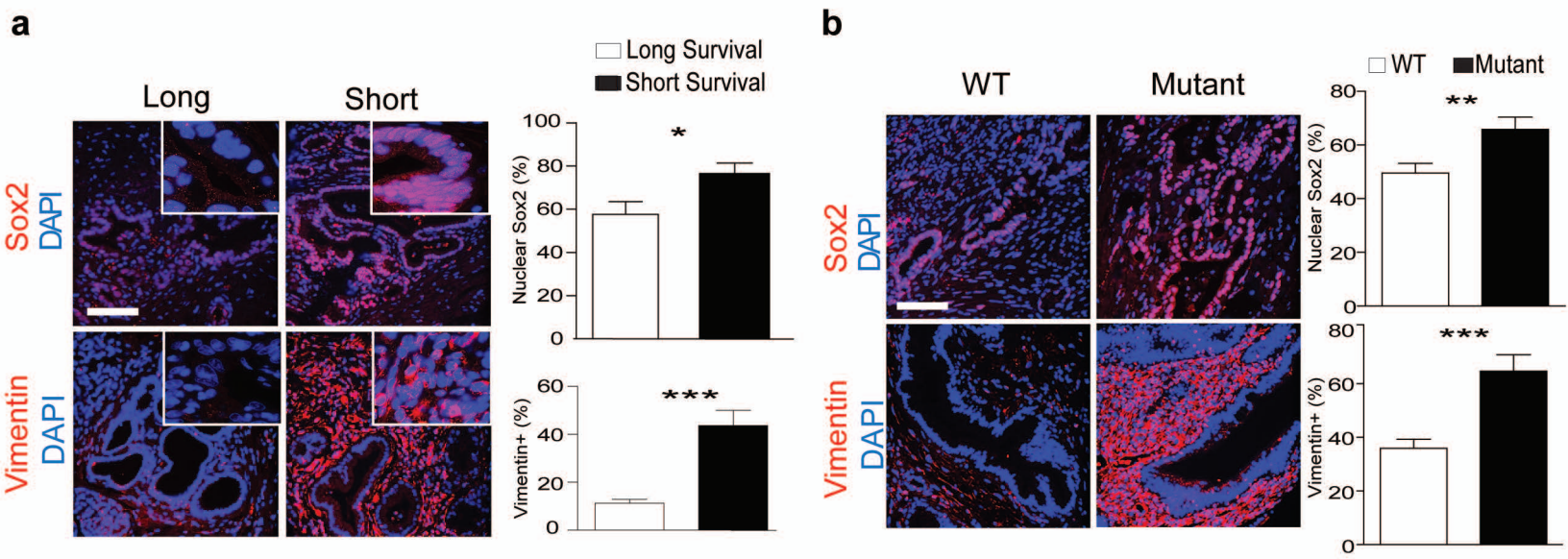

Supplementary Table 1

Individual Genes Used for Survival Analysis of GSE21501
COL1A2
COL2A1
COL3A1
COL4A1
COL5A1
COL11A1
COL24A1
COL27A1

Supplementary Table 2

Protein	Functional	Matrisome	MW	GENE	KPC/KC	p val	KTC/KC	p val	KTC/KPC	p val	Analytical CV(%)
Agrin(iso 2,3,4,5,&6)	Basement Membrane	Glycoprotein	208646	AGRN*	0.910	0.536	1.426	0.494	1.566	0.413	13%
Collagen alpha-1/5(IV) chain(Arresten/Core Protein)	Basement Membrane	Collagen	160613	COL4A1*	1.071	0.611	0.952	0.674	0.889	0.415	16%
Collagen alpha-1/5(IV) chain(Arresten/Core Protein)	Basement Membrane	Collagen	160613	COL4A1/5*	1.151	0.345	1.087	0.574	0.944	0.508	22%
Collagen alpha-2(IV) chain	Basement Membrane	Collagen	161386	COL4A2	1.047	0.735	1.065	0.669	1.017	0.844	14%
Collagen alpha-2(IV) chain(Canstatin/Core Protein)	Basement Membrane	Collagen	161386	COL4A2*	0.968	0.845	1.027	0.819	1.060	0.727	12%
Perlecan	Basement Membrane	Proteoglycan	375271	HSPG2	0.889	0.646	1.189	0.379	1.338	0.264	19%
Perlecan(Endorepellin)	Basement Membrane	Proteoglycan	375271	HSPG2*	0.908	0.712	0.958	0.827	1.055	0.860	7%
Laminin alpha-2	Basement Membrane	Glycoprotein	339982	LAMA2	1.108	ND	KC	ND	PC	ND	23%
Laminin alpha-5	Basement Membrane	Glycoprotein	404444	LAMA5	0.944	0.832	0.650	0.136	0.689	0.212	21%
Laminin Beta-1	Basement Membrane	Glycoprotein	197090	LAMB1	1.402	0.110	1.493	0.153	1.065	0.788	25%
Laminin Beta-2	Basement Membrane	Glycoprotein	196474	LAMB2	0.851	0.569	0.511	0.053	0.601	0.119	27%
Laminin Beta-3	Basement Membrane	Glycoprotein	128900	LAMB3	1.126	0.607	2.012	0.002	1.787	0.008	15%
Laminin Gamma-1	Basement Membrane	Glycoprotein	177387	LAMC1	0.881	0.389	1.054	0.775	1.197	0.351	ND
Laminin Gamma-2	Basement Membrane	Glycoprotein	130846	LAMC2	1.307	0.352	1.332	0.461	1.019	0.961	35%
Nidogen-1	Basement Membrane	Glycoprotein	137039	NID1	0.987	0.938	1.076	0.661	1.090	0.563	18%
Nidogen 1/2 (osteonidogen)(Nid1/2)	Basement Membrane	Glycoprotein	136538	NID1/2*	0.950	0.783	0.969	0.830	1.020	0.919	21%
Actin (All Isoforms)	Cytoskeletal	Cellular	42051	ACT	0.907	0.280	1.091	0.269	1.203	0.009	10%
Actin, cytoplasmic 1/2	Cytoskeletal	Cellular	41737	ACTB	1.139	0.300	1.271	0.128	1.116	0.497	10%
Desmin	Cytoskeletal	Cellular	53457	DES	0.515	0.373	0.257	0.163	0.499	0.338	12%
Spectrin alpha chain, non-erythrocytic 1	Cytoskeletal	Cellular	284637	SPTA2	1.143	0.400	0.984	0.928	0.861	0.280	20%
Tubulin beta-4B chain(4b & 5 chain)	Cytoskeletal	Cellular	49586	TUBB*	1.077	0.477	1.192	0.135	1.106	0.375	14%
Vimentin	Cytoskeletal	Cellular	53733	VIM	1.274	0.516	1.172	0.317	0.920	0.811	19%
Lysyl oxidase-like 1	ECM regulator	ECM regulator	66589	LOXL1	1.164	0.401	1.236	0.355	1.062	0.687	33%
Transglutaminase 2	ECM regulator	ECM regulator	77061	TGM2	1.017	0.829	0.669	0.013	0.657	0.001	11%
Collagen alpha-1(XII) chain	FACIT Collagen	Collagen	340214	COL12A1	0.782	0.421	1.724	0.171	2.203	0.097	13%
Collagen alpha-1(XIV) chain	FACIT Collagen	Collagen	191772	COL14A1	1.168	0.428	0.678	0.108	0.581	0.029	14%
Collagen alpha-1(I) chain	Fibrillar Collagen	Collagen	137953	COL1A1	0.911	0.250	0.916	0.529	1.005	0.969	10%
Collagen alpha-1(I) chain(C-term Propeptides (NC1 Domain))	Fibrillar Collagen	Collagen	137953	COL1A1*	1.002	0.979	1.365	0.133	1.363	0.128	12%
Collagen alpha-1(I) chain(fragment)	Fibrillar Collagen	Collagen	137953	COL1A1*	0.808	0.402	0.848	0.382	1.049	0.809	20%
Collagen alpha-2(I) chain	Fibrillar Collagen	Collagen	129564	COL1A2	0.931	0.393	1.036	0.801	1.112	0.465	14%
Collagen alpha-1(V) chain	Fibrillar Collagen	Collagen	183987	COL5A1	1.153	0.273	0.741	0.087	0.643	0.002	25%
Collagen alpha-2(V) chain	Fibrillar Collagen	Collagen	145018	COL5A2	0.997	0.987	0.759	0.295	0.762	0.125	11%
Collagen alpha-1(XVII) chain	Matricellular	Collagen	143568	COL17A1	1.009	0.968	1.594	0.173	1.580	0.114	26%
Collagen alpha-1(XVIII) chain	Matricellular	Collagen	182881	COL18A1	1.084	0.809	0.703	0.255	0.649	0.321	12%
Collagen alpha-1(VI) chain	Matricellular	Collagen	108806	COL6A1	0.980	0.938	0.574	0.081	0.586	0.117	15%
Collagen alpha-2(VI) chain	Matricellular	Collagen	108579	COL6A2	1.124	0.451	0.624	0.037	0.555	0.043	14%
Collagen alpha-3(VI) chain	Matricellular	Collagen	288133	COL6A3	0.730	0.314	0.391	0.002	0.535	0.244	16%
Collagen alpha-1(VII) chain(Fibronectin type-III 3 Domain)	Matricellular	Collagen	295092	COL7A1*	0.955	0.866	1.887	0.307	1.975	0.291	14%
Collagen alpha-1(VII) chain(Fibronectin type-III 1 Domain)	Matricellular	Collagen	295092	COL7A1*	1.001	0.972	1.882	0.318	1.879	0.176	25%
Dermatopontin	Matricellular	Glycoprotein	24203	DPT	1.281	0.176	0.757	0.101	0.591	0.025	11%
Fibulin 3	Matricellular	Glycoprotein	54596	EFEMP1	1.991	0.048	1.941	0.124	0.975	0.936	ND
Fibulin 4	Matricellular	Glycoprotein	44850	EFEMP2	0.754	0.366	1.423	0.031	1.887	0.063	14%
Emilin 1	Matricellular	Glycoprotein	106667	EMILIN1	1.042	0.658	0.889	0.265	0.853	0.156	17%
Fibulin 1	Matricellular	Glycoprotein	75381	FBLN1	1.349	0.183	2.678	0.052	1.985	0.093	34%
Fibronectin 1	Matricellular	Glycoprotein	272511	FN1	1.246	0.438	2.089	0.179	1.676	0.244	ND
Fibronectin 1(type-III 9 domain)	Matricellular	Glycoprotein	272511	FN1*	1.258	0.340	3.173	0.042	2.522	0.069	15%
Fibronectin 1(type-III 7 domain)	Matricellular	Glycoprotein	272511	FN1*	0.980	0.913	2.790	0.029	2.847	0.031	17%
Fibronectin 1(Anastellin/type-III 1 domain)	Matricellular	Glycoprotein	272511	FN1*	0.703	0.135	2.520	0.050	3.585	0.032	22%
Fibronectin 1(type-III 13 domain)	Matricellular	Glycoprotein	272511	FN1*	1.006	0.986	2.474	0.112	2.459	0.130	20%
Lumican	Matricellular	Proteoglycan	38279	LUM	1.092	0.106	0.983	0.888	0.900	0.393	9%
Periostin	Matricellular	Glycoprotein	93155	POSTN	0.831	0.086	1.300	0.369	1.563	0.191	15%
Prolargin	Matricellular	Proteoglycan	43179	PRELP	1.070	0.710	1.050	0.786	0.981	0.891	16%
Secreted protein, acidic, cysteine-rich (osteonectin)	Matricellular	Glycoprotein	34296	SPARC	1.280	0.513	1.366	0.109	1.068	0.827	15%
Osteopontin	Matricellular	Glycoprotein	34963	SPP1	0.794	0.360	1.193	0.451	1.503	0.174	14%
Thrombospondin 1	Matricellular	Glycoprotein	129647	THBS1	1.001	0.996	3.909	0.022	3.905	0.021	26%
tenascin C(Iso1,2,3,4,5)	Matricellular	Glycoprotein	221756	TNC*	1.052	0.927	4.324	0.033	4.112	0.036	14%
Versican	Matricellular	Proteoglycans	300008	VCAN	0.992	0.945	1.500	0.084	1.512	0.083	13%
Alpha/gamma-enolase	Other Cellular	Cellular	47128	ENO1/2	1.062	0.558	1.616	0.393	1.521	0.443	23%
Glyceraldehyde-3-phosphate dehydrogenase	Other Cellular	Cellular	35828	GAPDH	1.065	0.662	1.171	0.652	1.100	0.782	11%
Histone H1(H1.1,H1.2,H1.3,H1.4)	Other Cellular	Cellular	20863	H1*	1.178	0.433	0.780	0.133	0.662	0.080	9%
Histone 2A(H2A-A-K)	Other Cellular	Cellular	14077	H2A*	1.193	0.422	0.899	0.535	0.753	0.250	28%
Annexin A2	Other ECM	ECM-affiliated	38678	ANXA2	1.255	0.233	1.045	0.800	0.833	0.134	11%
Annexin A4	Other ECM	ECM-affiliated	35849	ANXA4	0.997	0.988	0.499	0.046	0.501	0.035	32%
Asporin	Other ECM	Proteoglycan	42573	ASPN	0.856	0.636	0.357	0.102	0.417	0.030	38%
Galectin-3	Other ECM	ECM-affiliated	27202	LGALS3	1.165	0.777	2.474	0.066	2.124	0.157	88%
Mimecan/Osteoglycin	Other ECM	Proteoglycan	34069	OGN	1.068	0.423	0.722	0.059	0.676	0.048	13%
Bone Marrow Proteoglycan(BMP & Eosinophil granule major basic protein)	Other ECM	Proteoglycan	25129	PRG2*	1.222	0.654	1.095	0.666	0.896	0.783	25%
Albumin	Secreted	Secreted	68731	ALB	0.945	0.671	1.093	0.604	1.156	0.442	13%
Transforming growth factor-beta-induced protein ig-h3	Secreted	Glycoprotein	74597	TGFBI	KC	ND	0.584	0.017	TC	ND	24%
Biglycan	Structural ECM	Proteoglycan	41706	BGN	1.175	0.285	1.682	0.021	1.431	0.079	10%
Decorin	Structural ECM	Proteoglycan	39805	DCN	1.345	0.007	0.764	0.017	0.568	0.000	19%
Fibrillin 1	Structural ECM	Glycoprotein	311952	FBN1	0.976	0.898	1.237	0.277	1.268	0.311	14%
Fibrillin 2	Structural ECM	Glycoprotein	313818	FBN2	1.059	0.694	1.129	0.778	1.066	0.881	21%
Fibromodulin	Structural ECM	Proteoglycan	43219	FMOD	0.813	0.500	1.601	0.008	1.970	0.036	21%
Latent transforming growth factor beta binding protein 1	Structural ECM	Glycoprotein	186599	LTBP1	0.897	0.647	1.917	0.138	2.137	0.127	ND
Microfibrillar-associated protein 2	Structural ECM	Glycoprotein	20578	MFAP2	1.024	0.822	1.033	0.791	1.009	0.950	13%

Supplementary Figure Legends

Supplementary Fig 1.

(**a**) Kaplan-Meier of overall survival of PDAC patients from GSE21501 with patients divided into those with high and low collagen expression by normalized microarray analysis of collagen gene expression, log rank $p = 0.04$, $n = 67$. (**b**) Bar graphs quantifying the Masson's Trichrome stained PDAC tissue arrays from patients with well ($n = 19$), moderately ($n = 23$) or poorly differentiated ($n = 26$) tumors. (**c**) Bar graphs quantifying the PR stained pancreatic tissue described in (b) within the main stroma. (**d**) Bar graphs quantifying the Masson's Trichrome stained PDAC tissue from PDAC patients cohort representing patients with a median short survival of 11−289 days (n=29) and median long survival of 1090−3298 days ($n = 28$). (**e**) Bar graphs quantifying the PR stained pancreatic tissue described in d within the main stroma. (**f**) Photomicrographs of Masson's Trichrome (top panel) stained PDAC tissue from PDAC patients cohort representing patients with wild type SMAD4 ($n = 10$) and mutant SMAD4 ($n = 10$). Scale bar, 100 μm. Immunofluorescence images and quantifications of pancreatic tissue as described above stained for αSMA (red, 2nd panel), and DAPI (blue). Scale bar, 75 μm. Results are presented as the mean +/- SEM. Subsequent statistical analysis was performed with unpaired two-sided student t-tests. (*$P < 0.05$; **$P < 0.01$, ***$P < 0.001$, ****$P < 0.0001$, "ns" not significant).

Supplementary Fig 2.

(**a**) Immunofluorescence images and quantifications of pancreatic tissues stained for Collagen 3 (green, 1st panel), FAP (green, 2nd panel), Gli1 (green, 3rd panel), αSMA (green, 4th panel) and DAPI (blue) from 20 weeks old tissue excised from mice expressing Kras with one mutant allele of *Tp53* (KPC) and Kras with heterozygous loss of the *Tgfbr2* in the pancreatic epithelium (KTC). Scale bar, 75 μm. For *in vivo* experiments, $n = 5$ mice per group. Subsequent statistical analysis was performed with unpaired two-sided student t-tests. (*$P < 0.05$; **$P < 0.01$, ***$P < 0.001$, ****$P < 0.0001$, "ns" not significant).

Supplementary Fig 3.

(**a**) Bar graphs quantifying the tissue images shown in the pancreatic tissue from 20 weeks old pancreatic tissue excised from mice expressing Kras (KC), Kras with one mutant allele of P53 (KPC) or Kras with heterozygous loss of *Tgfr2* in the pancreatic epithelium (KTC) shown in the

panels in figure (2a). (**b**) Bar graphs quantifying the matrix protein concentration of Tenascin C, Fibronectin 1 and collagen, type XII, alpha1 in KC and KTC tissues described above as measured by mass spectrometry. (**c**) Traction force maps measured on polyacrylamide gels (2,300 Pa) for isolated KC, KPC and KTC pancreatic epithelial tumor cells. For *in vitro* bar graphs, results are the mean +/- SEM of 3 independent experiments. For *in vivo* experiments, n = 5 mice per group. Subsequent statistical analysis was performed with unpaired two-sided student t-tests. (*$P < 0.05$; **$P < 0.01$, ***$P < 0.001$, ****$P < 0.0001$, "ns" not significant).

Supplementary Fig 4.

(**a**) Images of three dimensional collagen gels incubated with KC, KPC or with KTC pancreatic epithelial tumor cells treated with vehicle or the ROCK inhibitor Y27632. Cultures were assayed after 24 h (top panel). Polarized light images of color-coded PR stained collagen gels described above (bottom panel) and bar graphs quantifying three dimensional collagen gel contraction as indicated by collagen gel area shown in a. (**b**) Immunoblot and quantification showing Rock1 protein levels in KTC tumor cells expressing either a control shRNA or an shRNA to Rock1. Results are normalized to Gapdh. (**c**) Bar graphs quantifying the tissue images shown in the panels in figure (2e). (**d**) Bioluminescence images of tumor growth in nude mice 3 weeks after injection with KC, KPC, KTC and KTC pancreatic tumor cells expressing either a control shRNA or an shRNA to ROCK1. (**e**) Bar graph showing the weight of the pancreatic tumors generated by the KC, KPC and KTC pancreatic epithelial cancer cells. (**f**) Bar graphs quantifying CTGF mRNA expression for pancreatic tumors described in d. Results are normalized to β-actin. (**g**) Phase-contrast images of tumor colonies of KC, KPC, and KTC pancreatic tumor cells expressing either a control shRNA or an shRNA to ROCK1 embedded within soft agar. Scale bar, 40 μm and bar graph quantifying percentage of tumor colonies greater than 30 μm in diameter. For *in vitro* bar graphs, 3 technical replicates were performed and results are the mean +/- SEM of 3 independent experiments. For *in vivo* experiments, n = 5 mice per group. Subsequent statistical analysis was performed with either unpaired two-sided student t-tests, one-way ANOVA with Tukey's method for multiple comparisons. (*$P < 0.05$; **$P < 0.01$, ***$P < 0.001$, ****$P < 0.0001$, "ns" not significant).

Supplementary Fig 5.

(**a**) Images of collagen gels (top panel) and polarized light color-coded PR stained collagen gels (2^{nd} panel) incubated with KC or KPC pancreatic epithelial tumor cells treated with vehicle or

the Rock inhibitor Y27632 with accompanying quantifications. (**b**) Immunoblot and quantification showing Rock2 protein levels in KTC tumor cells expressing either a control shRNA or an shRNA to Rock2. Results are normalized to Gapdh. (**c**) Images of collagen gels incubated with KTC pancreatic tumor cells expressing either a control shRNA or an shRNA to Rock2 and quantifications. (**d**) Immunofluorescence images and quantifications of pancreatic epithelial tumor cells described in c stained for pMlc2 (red, top panel), pMyPT1 (red, 2nd panel) and DAPI (blue). Scale bar, 75 μm. For *in vitro* bar graphs, 3 technical replicates were performed and results are the mean +/- SEM of 3 independent experiments. Subsequent statistical analysis was performed with either unpaired two-sided student t-tests, one-way ANOVA with Tukey's method for multiple comparisons. (*P < 0.05; **P < 0.01, ***P < 0.001, ****P < 0.0001, "ns" not significant).

Supplementary Fig 6.

(**a**) Immunofluorescence images and quantifications of pancreatic tissue excised from 8 week old KC, KPC and KTC mice stained for pStat3 (red) and DAPI (blue). Scale bar, 50μm. (**b**) Representative images of three-dimensional collagen gels incubated with KTC pancreatic epithelial tumor cells for 24 hours either with vehicle or the JAK inhibitor Ruxolitinib. (**c**) Images of three-dimensional collagen gels incubated with KC tumor cells treated with vehicle or the conditioned media from 48 hour cultured KTC tumor cells treated with vehicle or with JAK inhibitor Ruxolitinib. (**d**) Immunoblot and quantification showing total (Stat3) and activated Stat3 (pStat3) levels in KTC tumor cells cultured on soft or stiff polyacrylamide substrates. (**e**) Cytokines array images measured in the conditioned media of KC and KTC cells cultured on soft or stiff polyacrylamide substrates. (f) Cartoon depicting the epithelial Jak-Rock-Stat3-Yap feed forward circuit and its potentiation by a stiff extracellular matrix microenvironment. For *in vitro* bar graphs, 3 technical replicates were performed and results are the mean +/- SEM of 3 independent experiments. For *in vivo* experiments, n = 5 mice per group. Subsequent statistical analysis was performed with either unpaired two-sided student t-tests, one-way ANOVA with Tukey's method for multiple comparisons. (*P < 0.05; **P < 0.01, ***P < 0.001, ****P < 0.0001, "ns" not significant).

Supplementary Fig 7.

(a) Graphic of mouse manipulations used to study the impact of β1-V737N expression in the pancreatic epithelium on tissue fibrosis. **(b)** Immunofluorescence images and quantifications of

pancreatic tissues excised from 3 month old control and β1-V737N mice stained for ^{p397}-Ptk2 (red, top panel) and p-MLC2 (red, 2nd panel), p-Stat3 (red, 5th panel), scale bar, 50 μm, CD45 (red, 6th panel) and CD68 (red, 7th panel), scale bar, 100 μm, and DAPI (blue). **(b)** (3rd panel) Polarized light images of collagen fibers revealed by picrosirius red (PR) staining of pancreatic tissue described above. Scale bar, 75 μm. **(b)** (4th panel) Representative force maps of ECM stiffness measured using AFM indentation in pancreatic tissue described above. **(c)** Bar graphs quantifying *Ctgf* mRNA expression for pancreatic tissue shown in (b). Results are normalized to β-actin. **(d)** Bar graphs showing quantification of total pancreatic CD45+ and Ly6C immune cells as determined by flow cytometry for pancreatic tissue shown in (b). **(e)**. Cytokines array images and quantification of measured in pancreatic tissue shown in b. For *in vitro* bar graphs, 3 technical replicates were performed and results are the mean +/- SEM of 3 independent experiments. For *in vivo* experiments, n = 5 mice per group. Subsequent statistical analysis was performed with either unpaired two-sided student t-tests, one-way ANOVA with Tukey's method for multiple comparisons. (*P < 0.05; **P < 0.01, ***P < 0.001, ****P < 0.0001, "ns" not significant).

Supplementary Fig 8.

(a) Immunofluorescence images and quantifications of 6 week old pancreatic tissue excised from β1-V737N mice treated with vehicle or the FAK inhibitor PND-1186 stained for ^{p397}-Ptk2 (red, top panel), p-MLC2 (red, 2nd panel), p-Stat3 (red, 5th panel), scale bar, 50 μm, CD45 (red, 6th panel), CD68 (red, 7th panel), scale bar, 100 μm, and DAPI (blue). (3rd panel) Polarized light images and quantification of collagen fibers revealed by PR staining of pancreatic tissue described above. Scale bar, 75 μm. (4th panel) Maps of ECM stiffness and quantifications measured using AFM indentation in pancreatic tissue described above. For *in vivo* experiments, n = 5 mice per group. Subsequent statistical analysis was performed with either unpaired two-sided student t-tests, one-way ANOVA with Tukey's method for multiple comparisons. (*P < 0.05; **P < 0.01, ***P < 0.001, ****P < 0.0001, "ns" not significant).

Supplementary Fig 9.

(**a**) Immunoblot showing FAK level in KTC tumor cells expressing either a control shRNA or an shRNA to Ptk2. Results are normalized to Gapdh. **(a')** Bar graph showing the quantification of a. (**b**) Representative bioluminescence images of tumor growth in nude mice 3 weeks after injection with KTC pancreatic tumor cells expressing either a control shRNA or an shRNA to

Ptk2. (**c**) Bar graphs showing KC and KC/β1-V737N mice body weight at study termination. (**d**) Bar graphs showing quantification of total pancreatic Ly6C and CD11b immune cells as determined by flow cytometry measured in KC and KC/β1-V737N pancreatic tissue. (**e**) Cytokines array images and quantifications measured in KC and KC/β1-V737N pancreatic tissue. For *in vitro* bar graphs, 3 technical replicates were performed and results are the mean +/- SEM of 3 independent experiments. For *in vivo* experiments, $n = 5$ mice per group. Subsequent statistical analysis was performed with either unpaired two-sided student t-tests, one-way ANOVA with Tukey's method for multiple comparisons. (*$P < 0.05$; **$P < 0.01$, ***$P < 0.001$, ****$P < 0.0001$, "ns" not significant).

Supplementary Fig 10.

(**a,b**) Polarized light images of collagen fibers revealed by PR staining of pancreatic tissues excised from 5 week old control, KC and homozygous KTC (KTC KO) mice (Top panel). Scale bar, 75 μm. Representative immunofluorescence images and quantifications of pancreatic tissues described above stained for p-MLC2 (red, 2nd panel), ^{p397}-Ptk2 (red, 3rd panel), YAP (red, 4th panel), p-Stat3 (red, 5th panel) and DAPI (blue). Scale bar 20 μm. (**c**) Quantification of ECM stiffness measured by AFM in pancreatic tissue shown in a. For *in vivo* experiments, $n = 5$ mice per group. Subsequent statistical analysis was performed with either unpaired two-sided student t-tests, one-way ANOVA with Tukey's method for multiple comparisons. (*$P < 0.05$; **$P < 0.01$, ***$P < 0.001$, ****$P < 0.0001$, "ns" not significant).

Supplementary Fig 11.

(**a**) Immunofluorescence images and quantifications of pancreatic tissues excised from 5 week old control and Stat3C mice stained for pStat3 (red, top panel), scale bar, 75 μm, ^{p397}-Ptk2 (red, 2nd panel) and pMlc2 (red, 3rd panel), scale bar, 50 μm, CD45 (red, 5th panel), CD68 (red, 6th panel), scale bar, 100 μm and DAPI (blue). Polarized light images of collagen fibers revealed by PR staining of pancreatic tissue described above (4th panel). Scale bar, 75 μm. Phase contrast images of H&E stained pancreatic tissue as described above (7th panel). Scale bar, 100 μm. (**b**) Bar graphs quantifying *Ctgf* mRNA expression for pancreatic tissue excised from 5 week old homozygous KTC (KTC KO) (Control) and KTC/Stat3 KO mice (Stat3 KO). Results are normalized to β-actin. (**c**) Immunofluorescence confocal images and quantifications of pancreatic tissues from 6 week old KTC (het) mice treated with either vehicle or the JAK inhibitor Ruxolitinib stained for pStat3 (red, top panel), scale bar, 75 μm, ^{p397}-Ptk2 (red, 2nd panel) and

pMlc2 (red, 3rd panel), scale bar, 50 µm, CD45 (red, 5th panel), CD68 (red, 6th panel), scale bar, 100 µm, and DAPI (blue). Polarized light images and quantifications of collagen fibers revealed by PR staining of pancreatic tissue described above (4th panel). Scale bar, 75 µm. Phase contrast images of H&E stained pancreatic tissue as described above (7th panel). Scale bar, 100 µm. (**d**) Quantification of ECM stiffness measured by AFM in pancreatic tissue shown in c. (**e**) Bar graphs quantifying the weight of the pancreatic tumors shown in c. For *in vivo* experiments, n = 5 mice per group. Subsequent statistical analysis was performed with either unpaired two-sided student t-tests, one-way ANOVA with Tukey's method for multiple comparisons. (*P < 0.05; **P < 0.01, ***P < 0.001, ****P < 0.0001, "ns" not significant).

Supplementary Fig 12.

(a) Immunofluorescence images and quantifications of pancreatic tissue from PDAC patients cohort representing patients with a median short survival of 11−289 days (n = 29) and median long survival of 1090−3298 days (n = 28) stained for Sox2 (red, top panel), Vimentin (red, 2nd panel) and DAPI (blue). Scale bar, 75 µm. **(b)** Immunofluorescence images and quantifications of pancreatic tissue from PDAC patients cohort representing patients with WT SMAD4 (n = 10) and mutant SMAD4 (n = 10) stained for Sox2 (red, top panel), Vimentin (red, 2nd panel) and DAPI (blue). Scale bar, 75 µm. Subsequent statistical analysis was performed with either unpaired two-sided student t-tests, one-way ANOVA with Tukey's method for multiple comparisons. (*P < 0.05; **P < 0.01, ***P < 0.001, ****P < 0.0001, "ns" not significant).

Supplementary Table 1.

List of genes used for gene expression analysis of human patient dataset GSE21501 presented in Supplmentary Figure 1a.

Supplementary Table 2.

Complete Mass spectrometry results from whole tissue analysis of ECM composition of KC, KPC, and KTC tumors (5 mice per group). Values are presented as a ratio of protein abundance between each of the groups as well as a statistical analysis of abundance differences.